A model for vibrations during dry sliding friction

A Model for Vibrations During Dry Sliding Friction

J. H. Dautzenberg (2) and J. A. G. Kals (1); Eindhoven University of Technology, Eindhoven/Netherlands

The occurrence of vibrations in tools during dry sliding friction is well known. A good understanding of this phenomenon leads to a better, possibly automatic, control of metal working operations. It is influenced by the dynamic characteristic of the equipment, machinery or test facility. In the present paper a relation for the acceleration of one of the sliding components is developed. The suggested model offers a physical explanation for the phenomenon of vibrations and screaming during dry sliding friction. It is based on plasticity theory and the surface geometry of the couple, as established from tests. Properties of the worn material are taken into account together with the dynamic characteristics of the experimental setup. With the normal force and the mass of the pinholder this leads to the frequency of the vibration. The friction tests have been carried out using a pin-ring setup on a lathe equipped with force and acceleration transducers. The experiments appear to support the model. The phenomenon described has been applied succesfully to detect the end of tool life in drilling experimentally.

1. INTRODUCTION.

In dry sliding friction at speeds of a few centimeters per second or faster, the generation of audible sound usually accompanies the sliding process. Such sounds are indictive of the presence of dynamic force fluctuations and motions in the contact region. In the past different authors have classified these vibrations. They distinguished three categories [1-4]:

- Stick slip.
  These vibrations, which occur when the sliding speed is sufficiently low, are periodic because the relative velocity between the surfaces is zero during the stick part of the cycle. The mechanism that causes stick-slip is attributed to the fact that the static and kinematic coefficients of friction are different.
- Vibrations induced by random surface irregularities.
  They occur at sufficiently low values of the normal load. The power spectral density of the oscillations exhibits a peak for each of the structural modes.
- Quasi-harmonic oscillations.
  These oscillations, which occur when the sliding speed and normal load are sufficiently high, are periodic and their waveform is nearly sinusoidal.

It has been shown that the course of the vibration characteristic can be used to predict the condition of machinery at the running stage of its life as well as for the breakdown time [5]. Besides that it has been experimentally confirmed and is adopted by an increasing number of researchers that friction implies plastic deformation [6-12]. This explains the surface geometry after dry friction as well as the metal microstructure, the deformation area near the contact zone and the conversion of mechanical energy in heat. This shows further the dependence on the penetration of deformation in the contact zone of a material property: the strain hardening [10,13].

Some time ago, Kramer [14] suggested to take the thermodynamic properties of the materials also into account. For he showed experimentally that the tool life in cutting, also being a plastic process [15,16], is influenced by the free enthalpy of material combinations of workpiece and tool material.

So, at least three different physical processes are important in dry friction. The present contribution relates the dynamic characteristics of the test facility with the plastic process. The tests have been performed on a pin-ring type sliding friction apparatus mounted on a lathe. For the modelling of the plastic process are the surface geometry of the ring and the plastic properties of the worn material relevant. It leads to a relation for the acceleration of one of the sliding components. The experiments appear to confirm the model. The measured forces usually have average values, the real momentary forces during contact, however, can be much higher. So, the ball bearings of the main spindle of the lathe appeared to be damaged after the test, although the average force values were rather low. Up to now the dynamic aspects of friction have been applied succesfully to detect the end of tool life in drilling experimentally as well as for the automatic quality control of stamped parts during the production process [17]. In both cases the sound and vibrations are appropriate as process variables for controlling the processes. The proposed model explains the vibrations and "screaming" during sliding friction.

In the following the model is presented. Further, the test apparatus is described and the experimental results are shown and discussed. Finally some conclusions are formulated.

2. MODEL.

Imagine a ring with N circumferential obstacles (width b and height h_o), which is pressed in a soft pin material with a shear flow stress τ. Fig. 1 shows this for one obstacle in a two dimensional representation. The relative sliding speed in x-direction is v_o (Fig. 2). Representing the friction process, the obstacle removes pin material by shearing in a cylindrical plane with radius R. From Fig. 1 it becomes clear that the removed material tends to press the pin away from the ring surface. The pin and pinholder with mass m, are elastically supported and can move in the pin axis direction (z-direction). It is pressed against the ring by a constant normal force F_N. The total power is:

$$P = \frac{v_o R N b \tau \sqrt{2h}}{\sqrt{R}} + \frac{F_N v_o \sqrt{2h}}{\sqrt{R}} + \frac{m v_o^2}{R} v_o \frac{R-h}{R} \sqrt{\frac{2h}{R}} \qquad (1)$$

where h is the penetration depth of the obstacle in the pin. The first term represents the plastic shearing power. The second is the power to shift the pin opposite to the constant normal force. The third represents the inertia power in order to accelerate the pin back. P has a minimum for:

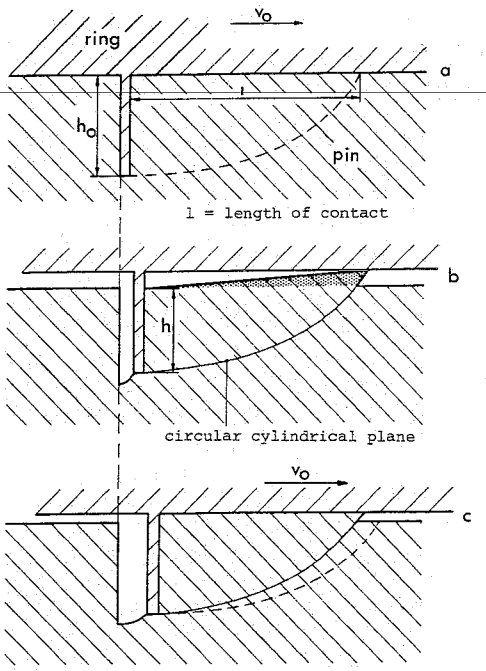

Fig. 1. Different successive shearing stages of the pinmaterial in a simplified reproduction.

$$\frac{dP}{dR} = 0 \qquad (2)$$

Hence, with Eqs. (1) and (2)

$$R = \frac{F_N + \sqrt{F_N^2 + 12 N b \tau m v_o^2}}{2 N b \tau} \qquad (3)$$

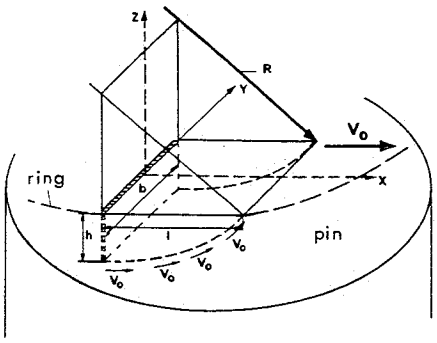

Fig. 2. A three dimensional representation of the deformation.

The acceleration in z-direction is:

$$a_z = \sqrt{\frac{Nb\tau v_o^2}{3m}} \qquad (4)$$

for

$$\frac{h}{R} << 1 \qquad (5)$$

and

$$F_N^2 << 12Nb\tau m v_o^2 \qquad (6)$$

Assuming that the material is spread in (compare Figs. 1b and 1c) and partly (1-f) squeezed out of the contact zone, for Eq. (4) becomes

$$a_z = \frac{1}{4} f^2 \sqrt{\frac{Nb\tau v_o^2}{3m}} \qquad (7)$$

However, the pin is only accelerated in the direction opposite to the ring as long as the obstacle of the ring makes contact with the pin. It is assumed that the penetration time equals the shift time: total contact time = $2t_o$. The time to restore the contact ($= 2t_L$) can be expressed as

$$2t_L = 2t_o \frac{F_N}{m} * \frac{1}{a_z} \qquad (8)$$

Fig. 3 represents the acceleration of the pin as a function of time. It is evident that a continuous repetition of this process is the vibration of the pin.

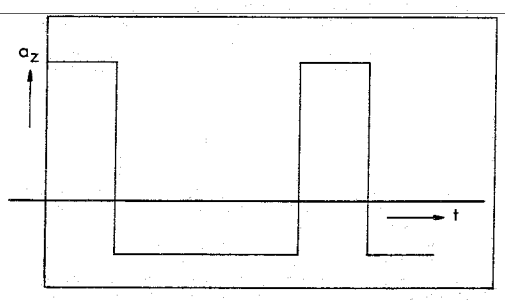

Fig. 3. Theoretical representation of the pin acceleration during dry sliding friction.

3. EXPERIMENTAL SETUP AND PROCEDURE.

The OFHC polycrystalline copper pins which were cylinders, 30 mm long and 8 mm in diameter, were vacuum annealed for 3h at 750°C and suited to the ring. The average grain diameter of the pin was between 10 and 15 μm. The rings were flat disks of normalized SAE 1045 steel, 80 mm in diameter and 10 mm thick, ground and finally polished with diamond paste. The pin with pinholder (Fig. 4) was pressed with air against the ring. The natural frequency of the pinholder in the normal force direction was 25 Hz [18]. The mass of pin and pinhilder (=m) was 0.86 kg. Pin and holder were clamped on a tube, which was hydrostatically borne. The friction force and the axial displacement of the pin, necessary for the wear rate calculations, were measured. The acceleration in the normal and friction dirctions was transformed with the aid of two small piezoelectric accelerometers on the pinholder near the pin. Signals have been visualized partly by a recording oscillograph (resonant frequency 15 kHz) and partly by a FFT analyzer. Test conditions were chosen in a way that merely displacement of copper could occur.

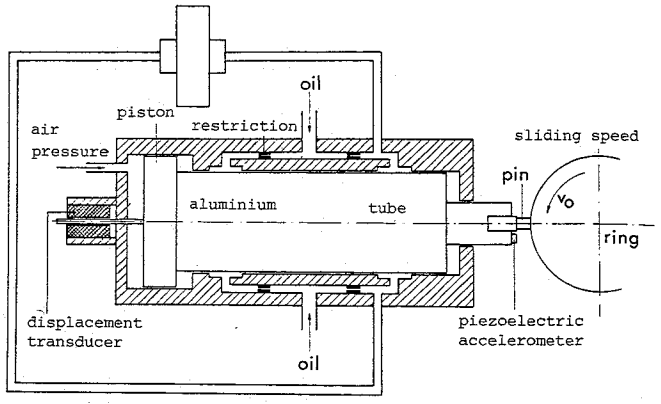

Fig. 4. The pinholder [18].

4. EXPERIMENTAL RESULTS.

Directly from the beginning the sliding contact causes irregular unevennesses arising from the outer ring surface. Fig. 5 shows a secondary electron image of such an obstacle. Fig. 6 is a section of a sliding couple perpendicular to the contact surface. Near the surface of the pin the bending of the grainboundaries in the sliding direction is visible. Fig. 7 shows a corresponding section of the pin from another experiment. It confirms the spreading of the copper and the existence of steps caused by the termination of momentary contacts. As in Fig. 6, but here more clearly, the deformation of copper is made visible. Fig. 8 shows the acceleration of the pin in z- (part A) and in x-direction (part B). In part A the times $2t_o$ and $2t_L$ are indicated. During t_L the calculated acceleration value F_N/m = 40 N/0.86 kg = 46.5 m/s^2 is in accordance with the experimental one. The shape of the acceleration signal during $2t_o$ is generally different in experiment (Fig. 8) and in theory (Fig. 3). This is attributed to the height- and width distribution of the obstacles on the ring. The acceleration a_z can be approximated by:

$$a_z = \ddot{z} = a_z^M (1 - t/t_o)^{2/3} \qquad (9)$$

with a_z^M = maximum acceleration in z-direction.

Double integration of Eq. (9) provides

$$h_o = \frac{3}{8} a_z^M t_o^2 \qquad (10)$$

where h_o = value of the highest obstacle during $2t_o$.

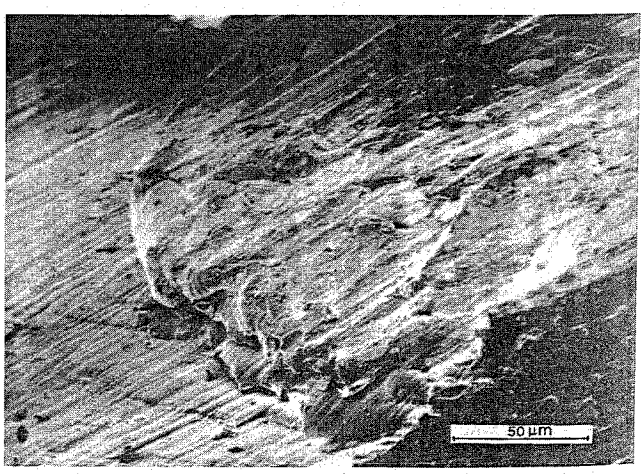

Fig. 5. Secondary electron image of an obstacle on a steel ring.

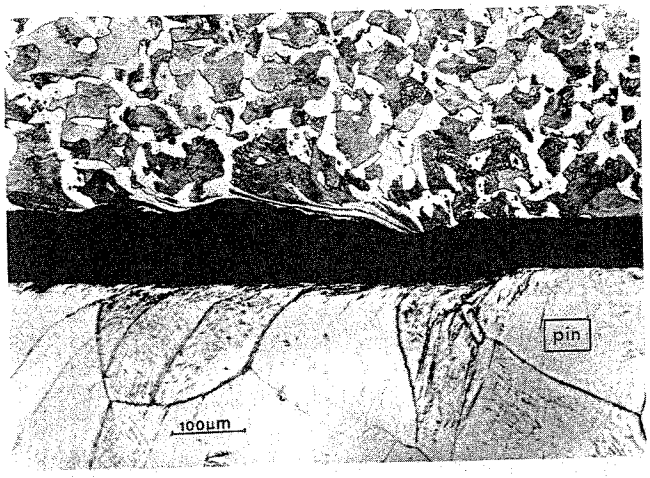

Fig. 6. Section of a sliding couple perpendicular to the contact surface and parallel to the friction force at low speed.

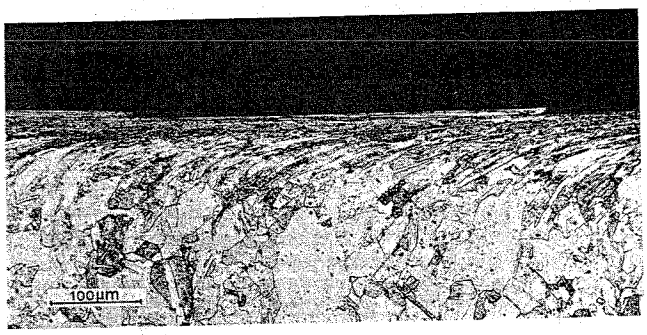

Fig. 7. Steps in a section of the copper pin perpendicular to the contact surface and parallel to the friction force at normal test speed.

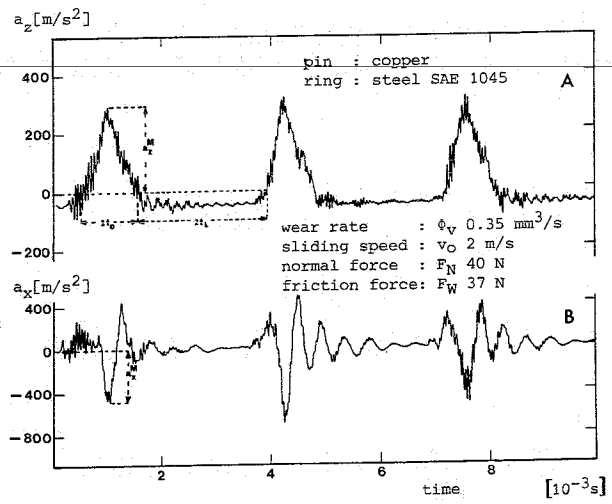

Fig. 8. The measured acceleration of the pin in axial direction (= a_z) and sliding direction (= a_x) as a function of time.

Table 1 presents the results of different tests under very different sliding conditions. It shows the influence of the normal force and sliding speed. Adjustment of a larger normal force causes generally a higher frequency. With Eq. (5) and f = 1 the number of contacts has been calculated. It is based on the assumptions that b = 200 µm, τ = 350 N/mm^2 and m = 0,86 kg. The table shows a decrease of contacts with increasing sliding speed. This may be caused by changing values of f and τ in reality, which are constant in the present calculations. Comparison of the times t_o and t_L indicates that the experimentally measured average friction force is much smaller than the momentary value.

Table 1. Experimental data of the sliding couple copper against steel SAE 1045.

F_N	v_o	F_W	Φ_V	a_z^M	a_x^M	ν	measured [$*10^{-4}$s]		h_o	N
[N]	[m/s]	[N]	[mm^3/s]	[m/s^2]	[m/s^2]	[s^{-1}]	t_o	t_L	[µm]	
10	0.5	13	0.015	83	99	275	5.0	13.2	7.8	17.0
10	6	14.3	0.39	81	162	282	3.5	14.2	3.7	0.1
40	0.5	22.5	0.082	189	277	497	3.55	6.5	8.9	84.0
40	2	39	0.315	260	421	343	4.1	10.5	16.4	10.0
40	4	38.5	1.08	307	1394	329	3.34	11.9	12.8	3.5
40	6	39.5	1.02	290	958	363	3.43	10.3	12.8	1.4
40	8	42.5	2.64	350	813	312	3.93	12.1	20.3	1.3
70	2	70	0.84	277	600	518	3.46	6.2	12.4	11.5
70	4	59	1.98	372	1024	428	3.14	8.5	13.8	5.2
70	6	65	3.3	366	927	410	3.4	8.8	15.9	2.2
70	8	68	5.28	349	912	440	3.3	8.1	14.3	1.1
100	2	96.5	0.96	258	1611	606	3.17	5.1	10.7	12.1
100	4	78.5	3.22	363	1076	537	2.72	6.6	10.6	5.5
100	6	86	4.7	383	1101	517	3.11	6.6	13.9	2.4
100	8	92.5	5.52	360	800	604	2.96	5.3	11.8	1.2
130	2	122.5	1.2	330	617	660	3.11	4.5	11.9	16.2
130	4	109	3.78	352	1117	673	2.4	5.0	7.6	4.6

F_N = normal force
v_o = sliding speed
F_W = friction force
Φ_V = wear rate

a_z^M = maximum of pin acceleration in z-direction

a_x^M = maximum of pin acceleration in x-direction
ν = pin frequency
$2t_o$ = contact time
$2t_L$ = restore time
h_o = obstacle height
N = number of contacts

Even during the short contact time it varies considerably. Substitution in Eq. (9) of t by $\frac{x}{v}$ and double integration leads to the path of the obstacle tip and thus to the shape formed in the pin surface. These shapes can be observed in the worn surface of a pin. Fig. 9 shows an example. It is measured with a Rank-Taylor Hobson apparatus.

The velocity obtained by simple geometrical integration of a_x in Fig. 8 is much smaller than the sliding speed; this means no stick-slip.

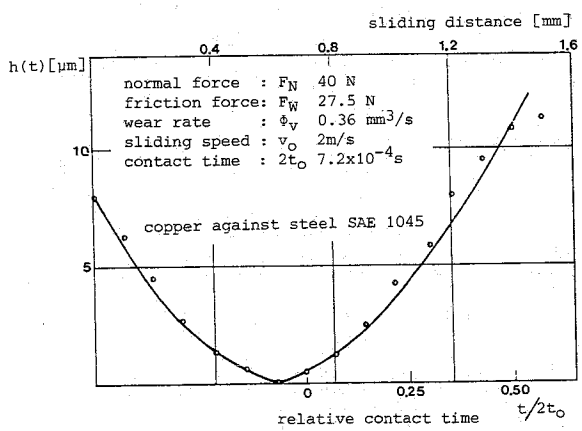

Fig. 9. A measured surface profile of a worn pin.

5. DISCUSSION.

- Eq. (4) is but valid under the condition expressed by Eq. (6). Table 2 elucidates Eq. (6) in giving the sliding speed for different values of the normal force.

- It proved true that the measured values for the height (h_o) of the obstacles are in agreement with the results obtained from Eq. (10). However, the active number of contacts cannot be taken from these height measurements. For both contact surfaces are rough.

- Quantitative analysis of the iron percentage in the virgin pin material (0.0035%) and the worn material (0.10 ± 0.03%) proves that new obstacles are formed and old are rubbed away continuously during friction. Obviously the obstacles work several times.

- Fig. 10A shows the acceleration in z-direction of the couple in the time domain. Fig. 10B gives the same signal in the frequency domain, and demonstrates only one frequency with its higher harmonics. Comparing Figs. 8 and 10 a difference in the magnitude of the acceleration can be pointed out. It may be caused by the use of a different steel for the test of Fig. 10.

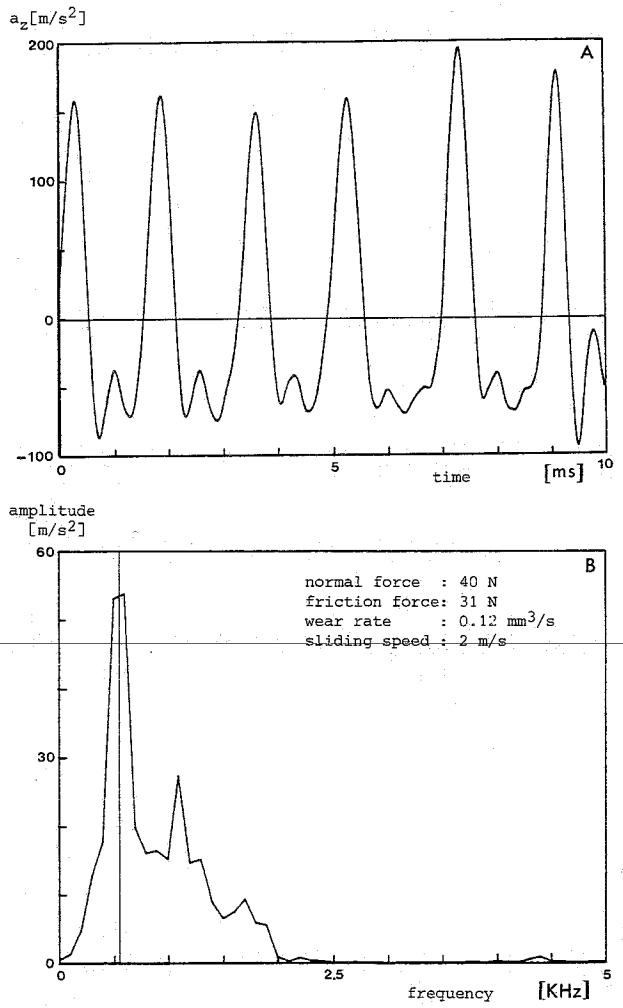

Fig. 10. The acceleration in z-direction in the time (A) and frequency (B) domain (bandwidth 5kHz).

- In [6] a lamination model has been used for calculating the wear rate. Laminates have also experimentally been demonstrated. They are generated by equal vibrations, as described in the present model.

- For the shear flow stress of copper in the contact zone the value of 350.16^6 N/m^2 is used. This value is discutable because the increasing effects of the large deformation and the large deformation rate, and the decreasing influence of the enhanced process temperature have been neglected. These effects in combination with a decreasing number of contacts and an increase of sliding speed can lead to a linear relation between a_z and v_o, as can be derived from Eq. (5), that is less pronounced (Table 1).

Table 2. Sliding speeds for which the acceleration is hardly depending on the normal force could be defined according to

$$\frac{F_N^2}{12mv_o^2Nb\tau} \ll 0.01 \text{ ;for example}$$

F_N[N]	N	v_o[m/s]
10	15	> 0.03
40	40	> 0.08
70	40	> 0.13
100	40	> 0.19
130	40	> 0.24

τ = critical shear stress (= 350 * 10^6 N/m^{-2})
b = track width (= 2 * 10^{-4}m)
m = mass of pin and pinholder (= 0.86 kg)
v_o = sliding speed
N = number of obstacles

- For the model we assumed that the shear plane is a part of a circular cylinder. Deviations cause as can be computed, higher values for the acceleration under the same test conditions.

- With Eq. (3) the contact area for one obstacle can be calculated.

- In the past the amplitude of the acceleration signal of the workpiece material during drilling has been used to detect the end of tool life. It has also been used to control the production of stamped parts [17]. Perhaps is will become possible to apply this method to watch the tool life in forming operations or the quality of parts. However, for both applications more research is neccesary.

- The model helps to understand the origin of the vibrations during dry sliding friction physically. It is based on the assumption that friction is a plastic deformation process and on the dynamic properties of the test machine.

6. CONCLUSIONS.

- A model has been made for the description of vibrations during dry sliding friction. Parameters are: the plastic properties of the sliding couple, the dynamic properties of the test machine and the dimensions and number of contacts on the ring surface.

- An analysis of the acceleration signal shows that the principal frequency is not an own frequency of the test machine.

- The height and number of obstacles on the ring can be deduced from the acceleration signal.

- The measured average forces are much smaller than the real forces during the contact time.

- The obstacles on the ring surface are continuously rubbed away and shaped again.

- It may be possible to use this effect for automatic production control.

- The model shows again that friction is a plastic deformation process. It is obviously a consequence of the plastic lamination model.

- The model provides a physical explanation for the phenomenon of vibration during dry sliding.

ACKNOWLEDGEMENT.

The authors are indebted to Messrs. J.A.B. van Dijck and M.J. Links for their experimental assistance.

REFERENCES.

[1] V. Aronov, A.F. D'Souza, S. Kalpakjian and I. Shareef. Experimental investigation of the effect of system rigidity on wear and friction-induced vibrations. ASME Journal of Lubrication Technology 105(1983)206-211.

[2] V. Aronov, A.F. D'Souza, S. Kalpakjian and I. Shareef. Interactions among friction, wear and system stiffness. Part 1-3, Journal of Lubrication Technology 106(1984)54-69.

[3] A. Soom and C. Kim: Interactions between dynamic normal and frictional forces during unlubricated sliding. ASME. Journal of Lubrication Technology 105(1983)221-229.

[4] A. Soom and C. Kim: Roughness-induced dynamic loading at dry and boundary-lubricated sliding contacts. ASME Journal of Lubrication Technology 105(1983)514-517.

[5] Cz. Cempel: The tribovibroacoustical model of machines. Wear 105(1985)297-305.

[6] J.H. Dautzenberg and J.H. Zaat. 1st European Tribology Congres C 276/73, September 1973, Institution Mechanical Engineers, London (1975).

[7] M.A. Moore. Proceedings International Conference on Wear of Materials 636-638, Dearborn 1979 ASME, New York (1979).

[8] N.P. Suh, S. Jahanmir, J. Fleming, E.P. Abrahamson, N. Saka, J.P. Teixeira. The delamination theory of wear II, Progress Report to ARPA, contract nr. 00014-67-A0204-0080. Nr. 229-011. September 1975.

[9] P.Heilmann and D.A. Rigney. An energy based model of friction and its application to coated systems. Wear 72(1981)195-217.

[10] J.H. Dautzenberg und J.A.G. Kals. Metallverformung bei trockener Reibung. Zeitschrift für Metallkunde 76(1985) 635-639.

[11] D. Kullman-Wildorf. Parametric theory of "adhesive" wear in uni-directional sliding. Proceedings: The international conference on wear of materials, Reston, Virginia ASME, 11-14 April 1983, 402-413.

[12] F.E. Kennedy and D.A. Voss. Proceedings: International conference on wear of materials II, Dearborn, 1979. ASME, New York, 89-96.

[13] J.H. Dautzenberg. Reibung und Gleitverschleiss bei Trockenreibung. Ph.D. Dissertation, Eindhoven University of Technology, Eindhoven, Netherlands (1977).

[14] P.D. Hartung and B.M. Kramer, submitted by B.F. von Turkovich (1). Tool wear in titanium machining. Annals of the CIRP 31/1(1982)75-80.

[15] J.H. Dautzenberg, J.A.G. Kals and A.C.H. van der Wolf. Forces and plastic work in cutting. Annals of the CIRP 32/1(1983)223-227.

[16] J.H. Dautzenberg and J. Vosmer. Cutting force relations for an arbitrary deformation model. Proceedings of the second conference of the Irish manufacturing committee, 4-5 september 1985. University of Ulster at Jordanstown, 207-218.

[17] F. Oppel und W. Ecker. Automatische Überwachung des Stanzvorganges durch Auswertung prozessbedingten Körperschalls. Technisches Messen 52(1985)411-416.

[18] H. Toersen. De drukgroepen en hydrostatisch gelagerde hoofdspil van de grote slijtageopstellingen. Eindhoven University of Technology, Department of Mechanical Engineering, Eindhoven, Netherlands WM-II-A-21 (1974).

(2) W.B.Ribbens and G.L.Lazik, "Use of optical data processing techniques for surface roughness studies," Proc.IEEE (Letters), Vol.56, pp.1637-1638, September 1968

(3) W.L.Anderson, "Surface roughness studies by optical processing methods", Proc.IEEE (Letters), Vol.57,P.95, October 1968

(4) J.W.Goodman, "Statistical properties of Laser speckle patterns", in "Laser speckle and related phenomena" edited by J.C.Dainty, Springer-Verlag, Berlin Heidelberg-New York, 1975.

PAPER N°4, Page 409 : M.LARACINE, C.BIGNON, M.BOIVIN, M.LORMAND/R.GESLOT
"Residual stresses measurement in plates by electro-chemical machining of fine layers"

Question from J.PETERS

- Quelle différence y a-t-il entre la méthode que vous proposez et la façon de procéder de nos collègues TOENSHOFF et BRINKSMEIER ?
- Etant donné l'électrolyte que vous utilisez et la brièveté du temps d'enlèvement de la couche, ne risquez vous pas de provoquer des déformations thermiques ou de relaxer les tensions que vous désirez mesurer ?

Réponse de M.LARACINE

- Le principe de base est le même, cependant avec notre système expérimental nous pouvons nous intéresser non seulement à la surface mais aussi déterminer le champ de contraintes résiduelles dans toute l'épaisseur de l'échantillon avec une mise en oeuvre relativement rapide et peu onéreuse.
- L'électrolyte thermostaté, circulant à grande vitesse ne saurait provoquer un échauffement à la surface de l'échantillon supérieur à 80°C. Compte tenu de la brièveté du temps d'usinage l'élévation de température dans la masse de l'échantillon reste négligeable et ne peut induire de traitement thermique. La stabilité de la valeur des déformations lues sur le pont de mesure après arrêt de l'usinage est le meilleur témoin de la stabilité de la température.

PAPER N°6, Page 417 : J.DAUTZENBERG (2), J.A.G.KALS (1)
"A model for vibrations during dry sliding friction"

Question from H.HINTERMANN

By using a pin-on-ring test rig you change the specific load continuously and hence also the conditions at the sliding interface. How does this influence your vibration mode and model ?

Answer from authors

The model presented is valid for instantaneous conditions. The shape of the acceleration vs.time curves as observed can only be explained on the basis of a continuously changing number of different active obstacles.
In this view the (specific)load is merely a result.

Question from P.VANHERCK

Your model is based on a soft and a hard material. What happens when using two materials with the same hardness?

Answer from authors

The combination as choosen represents not only the most common practical situation but is also accessible to analysis.

Question from J.PETERS

Considering the order of magnitude of the frquency you found, don't you think this phenomenon could not be the origin of the "hissing" noise we sometimes find in metal cutting ? It was an insolved problem in our former studies of the dynamic characterization of a material in relation to chatter. Don't you think your findings could bring some solution to that problem ?

Answer from authors

In our opinion, dry sliding friction as occurring between the rake face of the worn tool and the workpiece material could cause such vibrations. The model presented is also applicable in this case.

A D D E N D U M

CUTTING

PAPER N°9, Page63 : R.WERTHEIM (1), D.AGRANOV
"Wear behaviour of silicon nitride tools as a function of their specific properties"

Question from A.BER

What will happen to the thermal shock parameter (see fig.5) if the cutting speed is elevated from 300 m/min to a higher one ?
It can be suspected that an increase in the cutting speed v_c will decrease the thermal shock parameter rather than increase its values.

Answer from R.WERTHEIM

During machining with SiN and with higher cutting speeds, temperatures in the contact zone are higher than with common lower speeds. The thermal conductivity λ of SiN at higher cutting speed is lower than at room temperatures, for example, at room temperature pure SiN has approximately 18 W/m.K while at 1000°C an approximately 50% reduction can be expected. Thermal expansion α does increase at higher temperatures. There is also a slight reduction in strength at higher temperatures. Therefore the thermal shock parameter $R\lambda/\alpha$ in Fig. 5 which is calculated at room temperatures may be influenced in different ways for different materials compositions.
Compared to many other materials in which thermal conductivity increases with temperature, the values for SiN decrease at higher temperatures ; and therefore the material does act as an insulator. This may explain the improvement of tool life of SiN at higher cutting speeds compared to the behaviour of steels and cemented carbides.

Anonymous Question

What is the influence of different K land preparations on Silicon Nitride especially for turning machines ?

Answer from R.WERTHEIM

The influence of K-land geometry in turning differs from that in milling.It is also important to mention that one should distinguish between continuous turning and interrupted turning. For interrupted operations, the negative K-land with an angle of 20°-25° and width of 0,2 mm performs well in comparison to other tested geometries. For very low feeds of less than 0,1 mm/rev (or a tooth load of 0,1 mm/tooth), wear is higher than that of ceramics, due to higher specific loads as indicated in the paper and as reported by Prof. KOENIG (T.H.Aachen) during the STC meeting in Haifa.
For turning operationswith SiN insert, honed edges perform better than K-Land ; but again, the machining conditions and in particular the feed should be considered.
At the 1978 CIRP meeting Prof.LENZ reported that the angle of the chamfer (land) on Titanum Carbide inserts should be larger than 15° in order to reach reasonable tool life, which confirms with the results reported for the SiN-inserts.

FORMING

PAPER N°2, Page 141 : P.CHRISTENSEN, M.EVERFELT, N.BAY (2) T.WANHEIM
"Pressure distribution in plate rolling"

Question from Mr.AVITZUR

This is a fine treatment of the process of strip rolling analysing the effect of friction characteristics on the friction hill phenomenon, on roll torque and on the position of the neutral point.
The authors emphasize the use of proper description of the characteristics of friction, while employing an analysis by the free body equilibrium approach, in order to overcome some difficulties arising when on use the simpler friction models.
Is it possible that the difficulty in determining the position of the neutral point by the free body equilibrium approach is not due to the simplification in the simple friction model but due to a fundamental short coming in the use of the free body equilibrium approach ?
After all in the conventional application of the equilibrium approach, in the absence of front and back tension, the pressure at the entrance and exit, for non strain hardening material are equal. Thus, the friction hill suggests that the neutral point will never be at its exit, a situation that is nevertheless a reality when friction is too low and skidding occurs.

Answer from N.BAY

I do not agree that the slab method cannot result in a neutral point position at the exit. Dut to the roll curvature the normal stresses in the roll gap have a horizontal component acting backwards which will counteract the forward acting tangentional friction drag. Besides that, the conventional analyses use inappropriate boundary conditions assuming the normal pressure equal to the yield stress in plane strain so at the entry and exit. This is incorrect due to friction which should be taken into account. In our model this has been done using Mohr's circle and we are